Chemistry & Biology
Article

Consequences of Cisplatin Binding on Nucleosome Structure and Dynamics

Ryan C. Todd[1] and Stephen J. Lippard[1,*]
[1]Department of Chemistry, Massachusetts Institute of Technology, Cambridge, MA 02139, USA
*Correspondence: lippard@mit.edu
DOI 10.1016/j.chembiol.2010.10.018

SUMMARY

The effects of cisplatin binding to DNA were explored at the nucleosome level to incorporate key features of the eukaryotic nuclear environment. An X-ray crystal structure of a site-specifically platinated nucleosome carrying a 1,3-*cis*-{Pt(NH_3)$_2$}$^{2+}$-d(GpTpG) intrastrand cross-link reveals the details of how this adduct dictates the rotational positioning of DNA in the nucleosome. Results from in vitro nucleosome mobility assays indicate that a single platinum adduct interferes with ATP-independent sliding of DNA around the octamer core. Data from in vitro transcription experiments suggest that RNA polymerases can successfully navigate along cisplatin-damaged DNA templates that contain nucleosomes, but stall when the transcription elongation complex physically contacts a platinum cross-link located on the template strand. These results provide information about the effects of cisplatin binding to nuclear DNA and enhance our understanding of the mechanism of transcription inhibition by platinum anticancer compounds.

INTRODUCTION

Cisplatin, *cis*-diamminedichloroplatinum(II), is one of the most efficacious chemotherapeutic agents available in the battle against cancer. A curative treatment for testicular tumors (Loehrer and Einhorn, 1984), cisplatin was approved by the U.S. Food and Drug Administration in 1978. It is widely administered for several forms of cancer, being used inter alia to treat ovarian, cervical, head and neck, esophageal, and non-small-cell lung tumors (Keys et al., 1999; Loehrer and Einhorn, 1984; Morris et al., 1999). Only in testicular cancer, however, does the drug reach greater than 90% cure rates, approaching 100% in early stage cases (Bosl and Motzer, 1997). However, treatment can be limited by toxic side effects, including nephrotoxicity, emetogenesis, and neurotoxicity (Loehrer and Einhorn, 1984). Resistance to the drug, either acquired or inherent, is also common (Kartalou and Essigmann, 2001).

Since the serendipitous discovery of its antineoplastic activity (Rosenberg et al., 1965; Rosenberg et al., 1969), many research groups have focused on revealing the molecular details of the mechanism of action of cisplatin and related compounds. The early steps of triggering cell death by platinum(II) compounds involve four stages: (1) cellular accumulation by both passive and active uptake; (2) activation of the platinum(II) complex; (3) binding to nucleic acids to form a variety of Pt-DNA adducts; and (4) the cellular response to DNA damage (Jung and Lippard, 2007; Wang and Lippard, 2005). Cisplatin binds DNA at the N7 position of purine bases to form primarily 1,2-intrastrand adducts between adjacent guanosine residues (Cohen et al., 1980). A smaller number of 1,3-intrastrand, interstrand, and monofunctional Pt-DNA adducts also form. The DNA damage leads to disruption of several cellular processes, including transcription and replication. After cell cycle arrest, the Pt lesions are either removed by nucleotide excision repair (NER) or apoptosis is triggered.

DNA adducts of cisplatin have been thoroughly characterized by a variety of biochemical and biophysical methods, including X-ray crystallography and NMR spectroscopy, as previously reviewed (Jamieson and Lippard, 1999; Todd and Lippard, 2009; Wang and Lippard, 2005). However, one shortcoming of all such structural work is its failure to reproduce a key component of the eukaryotic cellular environment of nuclear DNA, namely, the nucleosome. DNA is packaged as chromatin, the building block of which is the nucleosome core particle (NCP). These protein-DNA complexes comprise ~146 base pairs of DNA wrapped in one and three-quarter turns as a left-handed superhelix around a core of eight histone proteins, two copies each of H2A, H2B, H3, and H4 (Kornberg and Lorch, 1999). These chromosomal proteins both provide a framework for condensing 2–3 m of human DNA into a compact structure that fits inside the nucleus of the cell, and they regulate DNA access by enzymes involved in replication, transcription, recombination, and repair (Workman, 2006). The location of nucleosomes in vivo is largely controlled by the intrinsic DNA sequence (Segal et al., 2006).

Despite the significant effort invested in studying interactions between cisplatin and DNA, very few reports exist in the literature discussing effects of platinum antitumor drug binding to chromatin or nucleosomes. Early studies revealed that *cis*- and *trans*-diamminedichloroplatinum(II) bind both histone-associated NCPs and free, linker DNA (Lippard and Hoeschele, 1979), there being a minor preference for linker DNA (Galea and Murray, 2002; Galea and Murray, 2010; Hayes and Scovell, 1991). More recent studies of platinum-nucleosome interactions have focused on structural effects of cisplatin binding to the NCP. Core particle DNA containing a site-specific cisplatin 1,2-d(GpG) or 1,3-d(GpTpG) intrastrand cross-link enforces a characteristic rotational orientation of the DNA strand on the nucleosome, such that the Pt adduct faces inward toward the

histone core (Danford et al., 2005; Ober and Lippard, 2007; Ober and Lippard, 2008). Such platinum-DNA cross-links are repaired less efficiently from nucleosomal compared to free DNA (Wang et al., 2003). These results suggest a mechanism by which platinum damage can be shielded from repair by the nucleosome surface. Other data indicate that platinum damage does not significantly affect the translational positioning of nucleosomes (Wu and Davey, 2008; Wu et al., 2008). Together, these results indicate that cisplatin adducts are located on NCP DNA in positions where they are readily accommodated by the nucleosome structure.

Although nucleosomes are inherently stable protein-DNA complexes, mechanisms exist that permit access of cellular proteins to the underlying DNA. The histone octamer can be translocated along DNA strands by either ATP-independent or -dependent pathways. In the former process, nucleosome sliding occurs in a temperature-dependent manner that reflects the stability of histone-DNA interactions for a given nucleosome (Luger, 2006; Pennings et al., 1991). In vivo nucleosome reorganization is directed primarily by ATP-dependent chromatin remodeling complexes (Flaus and Owen-Hughes, 2001) and histone chaperones (Park et al., 2005).

Proper nucleosomal positioning and mobility are critical to the fidelity of eukaryotic transcription (Workman, 2006). Initial transcription factor binding occurs at DNA promoter sites that are characteristically nucleosome-free, which allows the proteins to recognize and bind the exposed DNA sequence (Reinberg and Sims, 2006). Subsequent movement of transcription elongation complexes along nucleosomal DNA requires a mechanism for the advancing polymerase to overcome the octamer protein barrier. Bacteriophage T7 RNA polymerase (T7 RNAP) (Kirov et al., 1992; Studitsky et al., 1994; Studitsky et al., 1995) and eukaryotic RNA polymerase III (RNAP III) (Studitsky et al., 1997), but not RNA polymerase II (Kireeva et al., 2002), can transcribe nucleosomal DNA without removal of the histone octamer. The transcription elongation complex initially disrupts DNA-histone contacts ~20 base pairs ahead of the polymerase. As the complex reaches the nucleosome dyad, the octamer is displaced to a DNA region behind the RNA polymerase. During this process an intermediate loop forms, which is transcribed slowly and is perceived to be the rate-limiting step. Advancement of the polymerase along nucleosomal DNA induces rotational strain in the double helix, which is released through a twist diffusion mechanism. This mechanism is thought to be critical to the fidelity of nucleosome transcription (Gottesfeld et al., 2002; Mohammad-Rafiee et al., 2004). A series of DNA-binding pyrrole-imidazole ligands inhibit nucleic acid twist propagation and also block transcription by T7 RNAP from nucleosomal DNA, but not from free DNA. These results indicate a direct correlation between functional nucleosome mobility and successful transcription.

Inhibition of transcription by platinum-DNA damage has been investigated extensively, as reviewed elsewhere (Todd and Lippard, 2009); however, many of these studies were performed in vitro and utilized linear DNA, which does not account for nucleosome structure. There are three hypotheses about how cisplatin and its relatives inhibit transcription: (1) hijacking of transcription factors, (2) a physical block of the elongation complex, and (3) inhibition at the stage of chromatin remodeling (Todd and Lippard, 2009). Concerning the last theory, there are preliminary results indicating that globally platinated DNA inhibits histone translocation and propagation of twist diffusion in a manner similar to that for the aforementioned pyrrole-imidazole complexes (Wu and Davey, 2008). These data suggest a mechanism whereby cisplatin-DNA adducts may inhibit transcription by denying RNA polymerase elongation complexes access to nucleosomal DNA, but more research is necessary to test the validity of this hypothesis. Another study revealed cisplatin inhibition of both chromatin remodeling events and transcription, but no mechanistic connections were drawn between the two observations (Mymryk et al., 1995).

In the present report, we describe experiments performed to explore (1) how a single 1,2-*cis*-$\{Pt(NH_3)_2\}^{2+}$-d(GpG) or 1,3-*cis*-$\{Pt(NH_3)_2\}^{2+}$-d(GpTpG) intrastrand cross-link affects the structure of nucleosome core particles; (2) whether these Pt-DNA adducts inhibit DNA translocation and twist propagation; and (3) how elongation complexes of T7 RNAP navigate nucleosomes modified with site-specific cisplatin intrastrand lesions on either the template or coding strands. The X-ray crystal structure of a nucleosome core particle containing a single 1,3-*cis*-$\{Pt(NH_3)_2\}^{2+}$-d(GpTpG) intrastrand cross-link was determined. This adduct is commonly thought to be the major adduct of carboplatin (Blommaert et al., 1995), and it is more efficiently repaired than the corresponding 1,2-d(GpG) cross-link (Wang et al., 2003). Given the eukaryotic cellular environment and typical platination levels of DNA in cancer cells (~22 Pt per DNA molecule; Jamieson and Lippard, 1999), the mononucleosome model containing a single Pt-DNA cross-link provides the most physiologically relevant structural information about cisplatin-DNA modification to date.

ATP-independent nucleosome mobility, which requires propagation of rotational strain along the nucleosomal DNA (Luger, 2006), was measured by heat equilibration experiments, which monitor conversion of off-centered, kinetically formed NCPs to thermodynamically favored centered positions through histone translocation. To investigate transcription from platinum-damaged nucleosomes, DNA or nucleosome templates containing a 1,2-*cis*-$\{Pt(NH_3)_2\}^{2+}$-d(GpG) or 1,3-*cis*-$\{Pt(NH_3)_2\}^{2+}$-d(GpTpG) cross-link on either the template or coding strand were synthesized and subjected to single-round transcription assays by T7 RNAP. These results provided the first insight into the mechanism of transcription inhibition by Pt-DNA adducts in a nucleosome-containing environment. Data from these experiments allow us to evaluate the three hypotheses concerning the mechanism of transcription inhibition and draw useful conclusions.

RESULTS

Structure of the Platinated Nucleosome

The X-ray crystal structure of a nucleosome core particle, constructed from recombinant histone proteins and a synthetic 146-bp DNA duplex containing a 1,3-*cis*-$\{Pt(NH_3)_2\}^{2+}$-d(GpTpG) cross-link, was solved to an effective resolution (see Supplemental Experimental Procedures available online) of ~3.6 Å (Figure 1). The nucleosome accommodates the cisplatin adduct with no significant effect on the overall DNA or protein structure relative to that of the unmodified NCP. *N*-terminal tails of each

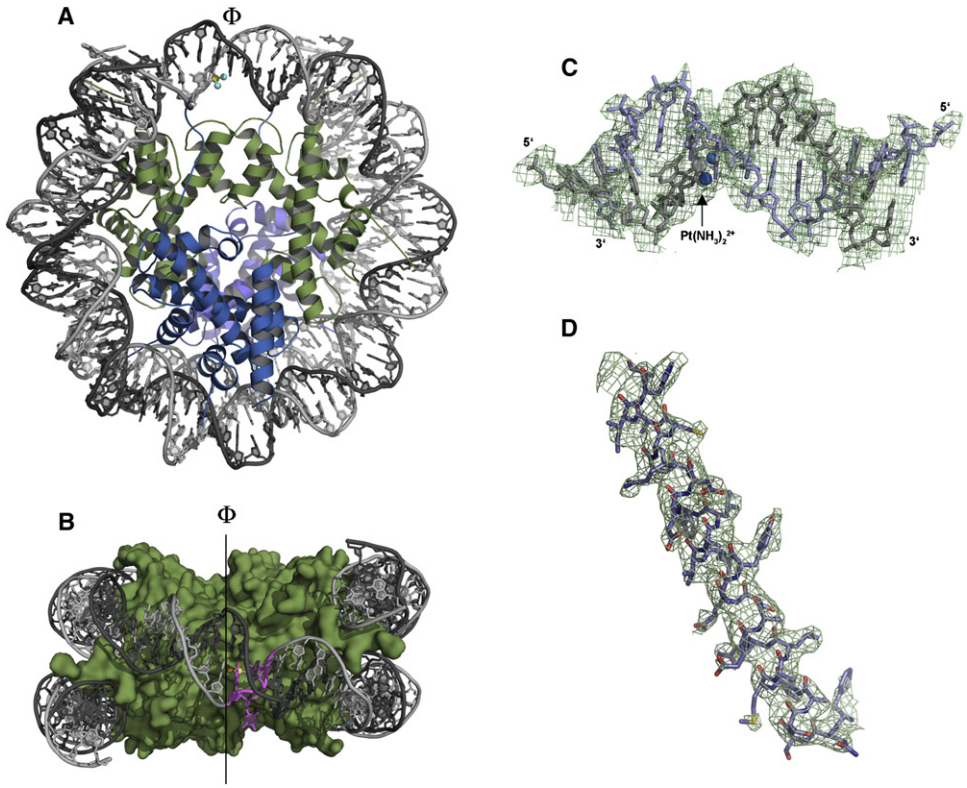

Figure 1. The Structure of the Platinum-Damaged Nucleosome Core Particle

(A) Overall NCP structure, which closely matches that of native nucleosomes. $(H3/H4)_2$ tetramer is shown in green, and H2A/H2B dimers in blue.

(B) Top view of the 1,3-*cis*-$\{Pt(NH_3)_2\}^{2+}$-d(GTG) cross-link (in purple/yellow). The dyad axis is marked by Φ.

(C and D) $2F_o$-F_c electron density maps surrounding the platinated DNA segment and an H3 α-helix, respectively. See also Figure S6.

histone are disordered and not visible in the structure, as is the case in almost all other nucleosome X-ray studies, and the octamer core geometry does not deviate from that of other nucleosomes incorporating *Xenopus laevis* histones. The DNA similarly adopts the same conformation with stabilizing hydrogen-bonding interactions primarily between histone arginine and lysine residues and the DNA phosphodiester backbone. These contacts occur at fourteen locations along the duplex, each time the minor groove contacts the octamer core.

The histone proteins are more ordered in the structure than the DNA superhelix, as can be judged from electron density maps in Figures 1C and 1D, as well as the average temperature factors. B-factors for all protein and DNA atoms averaged 101.5 A^2 and 219.9 A^2, respectively. The most ordered DNA bases are those in contact with the histone core, and the least ordered are those facing solvent, leading to a periodic distribution of temperature factors that is precisely out of phase for the two DNA strands (Figure S6). Watson-Crick base-pairing was restrained during the refinement, which aided the modeling of DNA regions facing the solvent for which the electron density was unclear. Although the DNA backbone, particularly the phosphodiester groups, and overall double helical structure are discernible (Figure 1C), individual base pairs are not resolved in the electron density, so their orientations could not be accurately determined.

Nucleosome core particles typically display two-fold pseudo-symmetry about a dyad axis that extends through the middle of the complex (Luger et al., 1997). NCPs can therefore pack into a crystal lattice in either of two possible orientations. Many nucleosome crystal structures incorporate a palindromic DNA sequence in order to circumvent this potential problem. In the present structure, both the DNA sequence and position of the 1,3-*cis*-$\{Pt(NH_3)_2\}^{2+}$-d(GpTpG) adduct are asymmetric with respect to the dyad, so both possible orientations could be present. An asymmetric nucleosome core particle has previously been studied by X-ray crystallography (Bao et al., 2006), but the resolution (3.2 Å) was notably lower than almost all other structures determined by the same research group. The resolution of the present structure similarly made location of the platinum adduct in initial refinement stages ambiguous and the DNA bases were not individually resolved. However, because the 1,3-*cis*-$\{Pt(NH_3)_2\}^{2+}$-d(GpTpG) cross-link was site-specifically engineered in the DNA duplex, placement of the adduct was limited to two possible positions. Moreover, the electron dense platinum atom afforded an additional clue to aid in the structure assignment.

In nucleosome core particles containing 146 bp DNA, one base pair falls directly on the dyad axis, splitting the DNA into "long" and "short" pieces containing 73 and 72 bp segments, respectively (Luger et al., 1997). Three NCP models were therefore prepared during refinement, one in which the cisplatin 1,3-intrastrand cross-link was placed on either the short or long DNA segment, and one in which no platinum moiety was

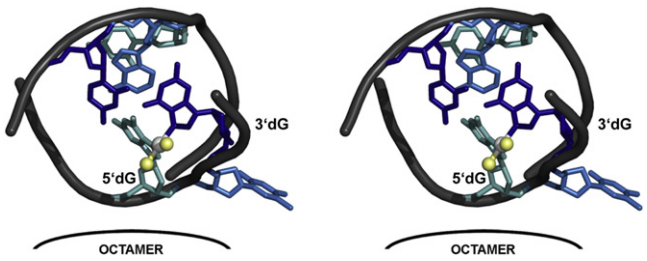

Figure 2. Stereo View of the 1,3-*cis*-{Pt(NH$_3$)$_2$}$^{2+}$-d(GpTpG) Cross-Link, Looking Down the DNA Double Helix

The location of the histone octamer is marked, showing how the cisplatin intrastrand adduct faces inward toward the protein core. See also Figure S7.

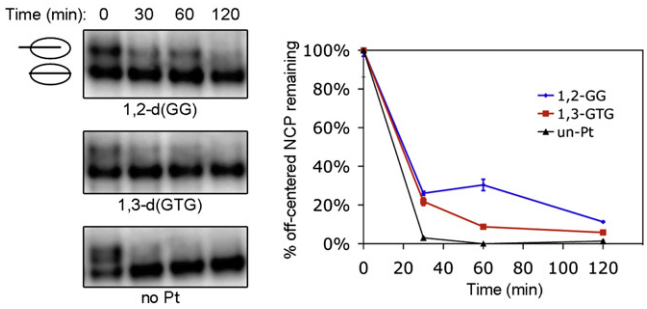

Figure 3. Mobility Study of Platinated Nucleosome Core Particles at 37°C

(Left) Native PAGE analysis of nucleosome mobility investigation of platinated nucleosome core particles at 37°C. The off-centered NCP (top band), a kinetic product, converts to the more thermodynamically stable centered nucleosome (lower band).

(Right) Quantitation of nucleosome mobility of platinated samples. Error bars represent the range of values observed.

included. Each model was refined by identical procedures. The R_{free} values for models without platinum, or with platinum on either the short or long DNA segment, were 30.9%, 30.6%, and 32.3%, respectively, indicating superiority for the orientation in which the 1,3-*cis*-{Pt(NH$_3$)$_2$}$^{2+}$-d(GpTpG) adduct is located on the 72 bp DNA half. This model and the one without platinum contained the same DNA sequence, the only difference being the presence or absence of a {Pt(NH$_3$)$_2$}$^{2+}$ unit. Because the entire DNA duplex in the two platinum-containing models was oriented differently, the separation in R_{free} values between the resulting structures was more dramatic. An F_o-F_c electron density difference map calculated from the model lacking platinum contained positive electron density at the appropriate site on the short DNA segment, but not at the other possible location, providing additional evidence that the proper orientation was chosen (Figure S7). Furthermore, a difference map calculated from the model containing the cisplatin adduct in the incorrect orientation on the long DNA half gave rise to a large negative peak surrounding the platinum atom. Together these data confirm that the cisplatin intrastrand cross-link location is properly determined in the reported nucleosome structure. Location of the platinum atom was also attempted by calculating anomalous difference Fourier maps using data collected at 1.072 Å (data not shown), but the single platinum atom provided an insufficient anomalous signal for its location.

The 1,3-*cis*-{Pt(NH$_3$)$_2$}$^{2+}$-d(GpTpG) cross-link faces inward toward the octamer and away from the solvent-exposed surface (Figures 1B and 2). This DNA rotational setting agrees with that predicted by chemical footprinting experiments (Ober and Lippard, 2007). No direct chemical interactions between the *cis*-{Pt(NH$_3$)$_2$}$^{2+}$ moiety and the octamer core are observed in the structure. One of the platinum ammine ligands sits ~5.0 Å from a lysine side-chain amino group, and these units can interact only by water-mediated hydrogen-bonding contacts, commonly observed at the DNA-histone surface (Davey et al., 2002). Details of the 1,3-*cis*-{Pt(NH$_3$)$_2$}$^{2+}$-d(GpTpG) adduct geometry also could not be discerned from the electron density, so Pt–N bond distances and angles were restrained during model refinement to values typical for platinum(II) square planar coordination compounds. In particular, little electron density for the internal thymine base of the d(GpTpG) unit is found; it is also disordered in NMR solution structures of platinated DNA (Teuben et al., 1999).

Nucleosome Mobility Investigation

The ability of a single cisplatin intrastrand cross-link to inhibit ATP-independent, heat-induced nucleosome mobility was explored. NCPs were prepared from DNA containing either no platinum, a 1,3-*cis*-{Pt(NH$_3$)$_2$}$^{2+}$-d(GpTpG) cross-link, or a 1,2-*cis*-{Pt(NH$_3$)$_2$}$^{2+}$-d(GpG) intrastrand adduct, respectively, and were subjected to heat equilibration at either 37°C or 50°C for a determined period of time (Figure 3). At 37°C, both cisplatin intrastrand cross-links inhibited DNA translocation. Unplatinated nucleosomes were completely shifted within 30 min at 37°C, whereas nucleosomes containing the 1,3-*cis*-{Pt(NH$_3$)$_2$}$^{2+}$-d(GpTpG) cross-link required 120 min to equilibrate fully at the same temperature. NCPs modified with a 1,2-Pt(GpG) intrastrand adduct still contained ~10% of nucleosomes at the off-centered translational position after 3 hr of heat equilibration, demonstrating that 1,2-Pt(GpG) intrastrand cross-links are better able to inhibit nucleosome mobility than their 1,3-Pt(GpTpG) counterpart. At 50°C, all nucleosome samples were completely equilibrated within 30 min (data not shown), indicating that the mechanism by which Pt-DNA cross-links inhibit the process does not involve covalent interactions between the platinum lesion and the protein core, nor any other irreversible phenomenon. These results are consistent with previous work demonstrating that nucleosome core particles globally treated with either cisplatin or oxaliplatin exhibit decreased nucleosome mobility (Wu and Davey, 2008).

Single-Round In Vitro Transcription Assays

Similarities between the abilities of cisplatin-DNA intrastrand cross-links and DNA minor groove-binding polyamide ligands to inhibit nucleosome sliding fuel the hypothesis that, like pyrrole-imidazole complexes, Pt-DNA adducts may block RNA synthesis by denying polymerase access to nucleosomal DNA and stalling the elongation complex at the histone octamer barrier. This idea was tested by single-round transcription assays of immobilized templates containing a defined nucleosome core particle site-specifically damaged by cisplatin.

Synthetic nucleosomes bearing centrally located cisplatin 1,2-d(GpG) or 1,3-d(GpTpG) intrastrand cross-link on either the

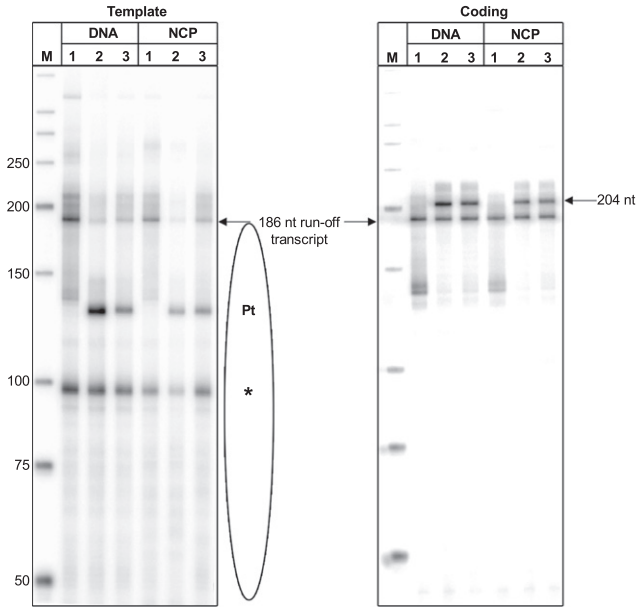

Figure 4. Transcription by T7 RNA Polymerase of 204-bp Templates

Templates contained free or nucleosomal DNA containing no platinum adduct (**1**), a 1,3-*cis*-Pt(GpTpG) cross-link (**2**), or a 1,2-*cis*-Pt(GpG) cross-link (**3**) on either the template (left) or coding strand (right). The oval represents area of the DNA covered by the nucleosome. Pt represents the location of the cross-link, and asterisk indicates the location of a native termination sequence. See also Figure S8.

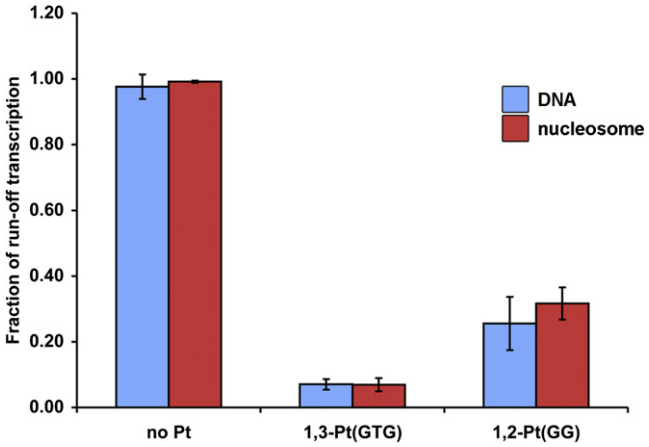

Figure 5. Quantitation of Transcription Inhibition by T7 RNA Polymerase from Site-Specific 1,3-*cis*-$\{Pt(NH_3)_2\}^{2+}$-d(GpTpG) or 1,2-*cis*-$\{Pt(NH_3)_2\}^{2+}$-d(GpG) Cross-Links

Blue bars represent transcription of DNA templates. Red bars represent transcription from nucleosomal templates. Error bars denote standard deviations of the reported values.

template or coding strand were prepared from 145-bp DNA with a 9-nucleotide overhang and recombinant histones. These constructs were annealed to a biotinylated 50-bp DNA fragment containing a T7 RNAP promoter and complementary overhang, ligated, and immobilized on streptavidin-coated magnetic beads. Assembling the nucleosomes initially on shorter DNA ensures a uniform translational position of the histone octamer on the transcription template. Nucleosome positions were assessed by restriction enzyme mapping of the DNA strand (Figures S4 and S5). The impact of a platinum cross-link on transcription elongation was determined by the ability of an elongation complex to transcribe off the DNA template, followed by analysis of the sites of inhibition.

Transcription results for constructs containing platinum on the template and coding strands are given in Figure 4. Kinetic analyses of transcription from the former strands were obtained, as depicted in Figure S8. Three primary products arise after transcription of DNA containing either a 1,3-*cis*-$\{Pt(NH_3)_2\}^{2+}$-d(GpTpG) cross-link, a 1,2-*cis*-$\{Pt(NH_3)_2\}^{2+}$-d(GpG) intrastrand cross-link, or no platinum damage on the template strand. These products are a 186-nt run-off transcript, a 124-nt product resulting from polymerase stalling at the site of the platinum adduct, and a third truncated product that appears at ~90 nt in all samples. Transcription efficiency was measured by comparing the relative amounts of the 124-nt terminated versus the 186-nt run-off transcript, as shown in Figure 5. Both the 1,3-d(GpTpG) and 1,2-d(GpG) cisplatin intrastrand cross-links strongly inhibit the T7 RNAP elongation complex at the site of the cross-link. The 1,3-cross-link is considerably more effective at blocking the enzyme than the 1,2-adduct. This trend was observed previously on free DNA with T7 RNA polymerase in similar systems (Jung and Lippard, 2003). The inherent termination product at 90 nt is the result of a T7 RNAP termination sequence, 5′-ATCTGTT-3′ on the nontemplate strand, a known inhibitor of the enzyme (He et al., 1998).

The same pattern of transcription inhibition occurs in free and nucleosomal DNA samples (compare blue and red bars, Figure 5). No shorter termination sequences arising from failure of the polymerase to navigate the nucleosome template were observed (see Figure 4; Figure S8). These results suggest that, although a single cisplatin intrastrand cross-link can inhibit DNA translocation along the histone octamer required for transcription of nucleosomal DNA by T7 RNAP, the elongation complex is able to overcome this barrier, and hence the effects of cisplatin on nucleosomal positioning are not a major determinant of T7 RNAP transcription inhibition. The physical adduct, however, is a much harder obstacle to overcome, and the polymerase is largely unable to transcribe through a platinum lesion placed on the template strand. A kinetic analysis of transcription of both free and nucleosomal DNA demonstrates that, under the conditions of this assay, there is no difference in rate of transcription from templates with or without a cisplatin damage site. The bacterial RNA polymerase can effectively transcribe through nucleosomal DNA even when the energy barrier to nucleosome translocation is increased.

Transcription of immobilized constructs with platinum cross-links on the nontemplate DNA strand yielded two major products, a run-off transcript and a longer template-sized product of 204 nt. Small amounts of RNA product were observed around 130 nt in length; these appear to arise from native termination sites because they are present in both sample sets, but the amount varied between experiments. No transcripts corresponding to inhibition at the site of the platinum adduct was observed because the cross-link was located on the nontemplate strand. The native termination site was also abolished

because the 5′-ATCTGTT-3′ sequence was removed from these strands. Finally, no transcripts arising from stalling of the elongation complex at the nucleosome barrier were observed. If platinum adducts blocked transcription through nucleosomes by prohibiting DNA twist diffusion and translocation around the histone core, then cross-links on both the template and coding strands would be equally effective at restricting access to nucleosomal DNA by the RNA polymerase.

DISCUSSION

Structural Analysis

The X-ray crystal structure of a nucleosome core particle modified with a specifically engineered 1,3-*cis*-$\{Pt(NH_3)_2\}^{2+}$-d(GpTpG) cross-link reveals interesting structural details about the effects of cisplatin-DNA damage. The Pt intrastrand cross-link is positioned near the dyad axis and faces the histone octamer core, in agreement with predictions of prior solution studies (Danford et al., 2005; Ober and Lippard, 2007). DNA near the platinum cross-link adopts a conformation similar to that of a free duplex having a centrally located 1,3-Pt(GpTpG) adduct, determined in solution by NMR spectroscopy (Teuben et al., 1999). The structure of an 11-bp DNA segment encompassing the Pt-DNA adduct (4 bp on both sides of the cross-link) was compared to that of the free DNA NMR solution structure containing the 1,3-*cis*-$\{Pt(NH_3)_2\}^{2+}$-d(GpTpG) cross-link. The helical bend angles for the nucleosomal and free DNA segments are 39.1° and 45.4°, respectively, indicating that the local nucleic acid structure around the nucleosomal Pt adduct mimics its solution-state form in a free DNA duplex. These angles were calculated using the program Curves+, with the NMR value deviating by 9 ± 3° (Teuben et al., 1999) from that reported in the original publication. This discrepancy arises from known differences in calculating global DNA structure parameters (Lavery et al., 2009).

Our results suggest a mechanism by which cisplatin intrastrand cross-links, after covalent binding to nucleosomal DNA, might afford a rotational setting that accommodates structural deviations caused by the bifunctional adduct. Superhelical DNA in the nucleosome is highly distorted, and the data presented here indicate that Pt-DNA adducts alter the DNA position in the nucleosome such that the bend induced by a platinum 1,3-intrastrand cross-link is congruent with the bend caused by wrapping of DNA around the histone core. Bending of nucleosomal DNA is centralized in both the major and minor grooves, alternating in ~5-bp patterns (Figure S9). It is therefore more favorable for the cisplatin cross-link, which causes DNA bending toward the major groove, to be located at a position on the nucleosome where the superhelical bend is also directed toward the major groove. Further evidence to support this conclusion is provided by the observation that nucleosome core particles treated with cisplatin or oxaliplatin form DNA adducts preferentially at locations where the purine bases already experience a large roll angle due to the superhelical structure (Wu et al., 2008). However, it is unlikely that platinum would initially bind in these locations, because the reactive aquated species will more likely react at a surface-exposed purine base. Also, because the bifunctional cross-link is formed in a stepwise manner (Bancroft et al., 1990), the initial monofunctional cisplatin adduct would a priori have no preferred DNA bend. Thus location of the cisplatin cross-link at its preferred nucleosome position most likely involves a rearrangement that occurs after the formation of the cross-link.

A more in-depth analysis of the cisplatin-modified nucleosome core particle structure is limited by the ~3.6 Å effective resolution, affording insufficient electron density in regions of the DNA and platinum intrastrand cross-link. Because the DNA sequence is nonpalindromic and the Pt-DNA adduct is asymmetric with respect to the nucleosome dyad, packing of NCPs within the crystal lattice is less efficient than might occur with a more symmetric construct. An asymmetric nucleosome structure has been solved previously (Bao et al., 2006), but this structure is also limited by resolution. The refined temperature factors in the present structure are high, but comparable to those obtained for other nucleosome core particles at similar resolution (Bao et al., 2006; Wu et al., 2008).

Effects of Platination on Nucleosome Sliding

Inspection of heat-induced gel mobility shifts of the platinated mononucleosomes reveals that, like nucleosomal DNA-bound polyamide complexes (Gottesfeld et al., 2002), NCPs bearing cisplatin intrastrand cross-links inhibit DNA translocation along the histone octamer. Polyamides block transcription of nucleosomal but not linear DNA, leading to the hypothesis that these adducts lock the nucleosome in place and prevent DNA sliding. This process is proposed to occur by inhibiting DNA twist diffusion. Similarly, cisplatin-DNA cross-links have a highly preferred relative location on nucleosomal DNA, where the adduct faces inward toward the core, which conveys upon them a propensity to inhibit thermal translocation. Movement of the histone core along platinum-modified DNA would force bent Pt-DNA region out of phase with the superhelical bend, a disfavored process. The cisplatin 1,2-d(GpG) cross-links cause a more dramatic bend angle than 1,3-d(GpTpG) cross-links (Gelasco and Lippard, 1998; Teuben et al., 1999), and are a slightly stronger inhibitor of DNA sliding. However, the magnitude of this effect from a single cisplatin adduct is smaller than that from both the pyrrole-imidazole ligands (Gottesfeld et al., 2002) and from multiple Pt lesions (Wu and Davey, 2008). We therefore cannot conclude from these data alone that a single Pt cross-link will inhibit transcription by this mechanism analogously to polyamide ligands.

Transcription Inhibition of Platinated Nucleosomes

Of the three current hypotheses presented in the Introduction describing how platinum intrastrand cross-links may inhibit transcription in cancer cells (Todd and Lippard, 2009), the results of our in vitro transcription experiments argue against disruption of nucleosome dynamics as a potential mechanism. They provide further evidence to support the hypothesis that DNA adducts of these compounds physically prevent translocation of the RNA polymerase elongation complex, even in a eukaryotic nucleosome environment. Although a single $\{Pt(NH_3)_2\}^{2+}$ intrastrand cross-link reduces the rate of nucleosome mobility to some degree, this effect appears to be insufficient to prevent the histone translocation that occurs during transcription of nucleosomes by T7 RNA polymerase, or, by analogy, RNA polymerase III. Further experiments are needed to determine the

consequences of decreased NCP mobility by Pt-DNA damage on transcription by RNA polymerase II, which involves remodeling coenzymes.

An interesting side-product of transcription reactions on templates containing platinum cross-links on the DNA coding strand of either free or nucleosomal templates is a transcript longer than the run-off product, ~204 nt in length. This value corresponds to the full length of the DNA template, including the promoter site, and is not observed in either unplatinated samples or sample containing Pt adducts on the template strand. T7 RNAP transcripts longer than the run-off length have been observed previously, (Macdonald et al., 1993; Nacheva and Berzal-Herranz, 2003; Rong et al., 1998), including template-sized side products (Schenborn and Mierendorf, 1985). At present it is unclear why a longer RNA product appears in transcription reactions utilizing DNA templates with platinum cross-links on the coding strand.

SIGNIFICANCE

We investigated the effects of a single defined cisplatin intrastrand cross-link on nucleosome structure and dynamics. An X-ray crystal structure reveals that a 1,3-d(GpTpG) cross-link determines the rotational phasing of nucleosomal DNA such that the major groove bending caused by platinum binding aligns with the distortion of the DNA superhelix. This preferred location also moderately inhibits nucleosome sliding, as determined by measurements of heat-induced mobility. Finally, we demonstrate that, despite limiting nucleosome mobility, platinum-damaged nucleosomes are readily transcribed by bacterial RNA polymerases, which arrest at the site of a cisplatin adduct on the DNA template strand. These data provide insights into the structural and mechanistic consequences of cisplatin-DNA binding in a eukaryotic environment and reveal details of the mechanism of transcription inhibition by this potent anticancer drug.

EXPERIMENTAL PROCEDURES

Materials

Phosphoramidites, columns, and other reagents for solid-phase oligonucleotide synthesis were purchased from Glen Research. Potassium tetrachloroplatinate(II) used to prepare cisplatin (Dhara, 1970) was a gift from Engelhard Corporation (now BASF). Enzymes were purchased from New England Biolabs. γ-^{32}P-ATP and α-^{32}P-GTP (6000 Ci/mmol) were purchased from Perkin Elmer. Dynabead M-280 streptavidin-coated magnetic beads were purchased from Invitrogen. All other reagents were purchased from commercial suppliers and used without further purification. Dialyses were performed using Spectra/Por dialysis membranes of an appropriate molecular weight cut-off and were pretreated with hot 50 mM aqueous EDTA, followed by several washes with water and dialysis buffer, prior to use. Radioactive gels were visualized using a Storm 840 phosphorimager, and sample radioactivity was quantitated with a Beckman LS 6500 scintillation counter. All nucleosome gels were run on 4.5% native PAGE (0.3× TBE, 37.5:1 mono:bis acrylamide) in a cold room at 4°C.

Synthesis of Site-Specifically Platinated DNA Duplexes

Double-stranded DNA duplexes containing site-specific $\{Pt(NH_3)_2\}^{2+}$ modifications were prepared by ligation of five synthetic oligonucleotides as previously described (Ober and Lippard, 2007). Oligonucleotide sequences of the individual strands for each duplex are provided in the Supplemental Experimental Procedures. DNA in nucleosomes for crystallization and mobility experiments contained 146-bp DNA and either no platinum cross-link (**t1**), a 1,3-*cis*-$\{Pt(NH_3)_2\}^{2+}$-d(GpTpG) intrastrand cross-link (**t1-Pt**), or a 1,2-*cis*-$\{Pt(NH_3)_2\}^{2+}$-d(GpG) lesion (**t2-Pt**). For transcription experiments, 145-bp DNA was prepared with a 9-nt overhang to allow subsequent ligation to a T7-promoter-containing DNA fragment. DNA strands were prepared in which a 1,3-*cis*-$\{Pt(NH_3)_2\}^{2+}$-d(GpTpG) intrastrand cross-link or 1,2-*cis*-$\{Pt(NH_3)_2\}^{2+}$-d(GpG) lesion was engineered into the template (**s1-Pt** and **s2-Pt**, respectively) or coding strand (**c1-Pt** and **c2-Pt**, respectively) of the DNA duplex. Corresponding duplexes in which no platinum modification was introduced were also prepared, referred to as **s1**, **s2**, **c1**, and **c2**, respectively.

Nucleosome Reconstitution

Nucleosomes were assembled by dialysis at 4°C with synthetic DNA duplexes and octamer cores containing recombinant histone proteins (*X. laevis*, expressed in *Escherichia coli*) in a 0.9:1 ratio as previously described (Dyer et al., 2004). Nucleosomes for crystallization were reconstituted on a 1-5 nmol scale with a DNA concentration of ~0.7 mg/mL and were purified by preparative gel electrophoresis, as described elsewhere (Dyer et al., 2004). Nucleosomes for transcription experiments were prepared on a 20 pmol scale in microdialysis buttons that were constructed from the cap of a 200 μl polymerase chain reaction tube and a 1 cm^2 Spectra/Por MWCO 6–8 kDa dialysis membrane (Thåström et al., 2004), and used without further purification. The amount of free DNA remaining in solution was quantitated by analytical PAGE with ethidium bromide staining.

Nucleosome Structure Determination

Diffraction-quality crystals of nucleosomes containing the cisplatin 1,3-cis-$\{Pt(NH_3)_2\}^{2+}$-d(GpTpG) intrastrand cross-link were grown by sitting-drop vapor diffusion under conditions described in previous nucleosome structural studies (Luger et al., 1997). Details of crystallization, data collection and processing, and structure refinement are found in the Supplemental Experimental Procedures.

Nucleosome Mobility Investigation

^{32}P-Labeled **t1**, **t1-Pt**, or **t2-Pt** strands (40 pmol) were combined with an equimolar amount of histone cores in 20 μl of buffer containing 2 M KCl, and nucleosomes were prepared by dialysis as described elsewhere (Dyer et al., 2004). All samples were prepared in duplicate. Following dialysis, the volume of each sample was brought to 50 μL, and a 20 μl portion of each was incubated at 37°C or 50°C. The remaining 10 μl was kept at 4°C. Aliquots of each sample were taken at 30, 60, 120, and 180 min, and the radioactivity was quantified by scintillation counting. Samples were analyzed by 4.5% native PAGE.

Preparation of 204 bp Immobilized Transcription Templates

A biotinylated and radiolabeled promoter fragment containing the T7 RNA polymerase promoter site was prepared by combining 100 pmol each of 5′-^{32}P-labeled **f** and 5′-phosphorylated **bio-g** (sequences in Supplemental Experimental Procedures), annealing from 80°C to 4°C over 2.5 hr using a constant temperature gradient, and purifying by 5% native PAGE. For transcription experiments, unlabeled DNA was utilized. The promoter fragment (2 pmol) was ligated with an equimolar portion of either DNA or NCP with sequence **s1**, **s1-Pt**, **s2-Pt**, **c1**, **c1-Pt**, or **c2-Pt** in 100 μl solution (50 mM Tris/HCl [pH 7.5], 10 mM $MgCl_2$, 1 mM ATP, 10 mM DTT, 0.5 mg/mL BSA, 1% PEG-8000, and 0.4 U/μL T4 DNA ligase) at 16°C for 2 hr. Samples were heated to 50°C for 10 min to deactivate the enzyme. Separately, 1.5 mg of Dynabead M-280 streptavidin-coated magnetic beads were washed two times each with 200 μl of 0.1 M NaOH, 50 mM NaCl in diethylpyrocarbonate (DEPC)–treated water, then 100 mM NaCl in DEPC-treated water to make suitable for RNA applications. Beads were then washed twice each with bind/wash buffer (2 M NaCl, 10 mM Tris/HCl [pH 7.5], and 1 mM EDTA) and TE600 buffer (600 mM NaCl, 10 mM Tris/HCl [pH 7.5], and 1 mM EDTA), then resuspended in 750 μl of TE600. Washing was performed by suspending the sample by pipette mixing, then collecting the beads with a magnet and removing the supernatant. After deactivation of the T4 DNA ligase, a 100-μl aliquot of streptavidin beads was added to each sample, mixed by pipette, and incubated at room temperature for 30 min with gentle rocking to allow binding of the biotinylated DNA constructs. Unbound material was removed

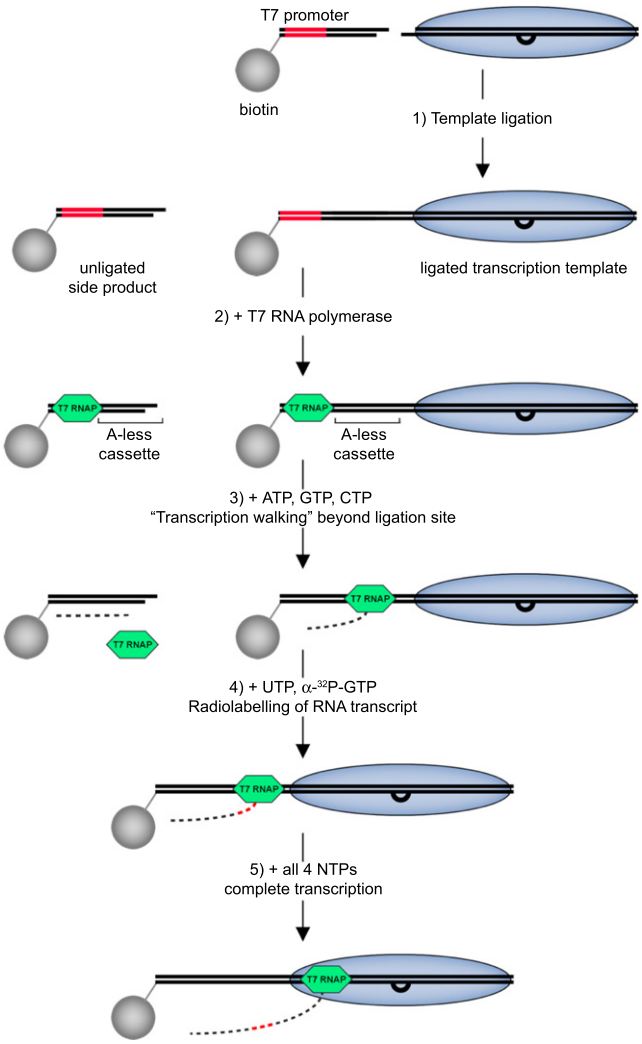

Figure 6. Experimental System Using Immobilized Free or Nucleosomal Templates to Study Transcription by T7 RNA Polymerase

Elongation complexes are formed on a mixture of fully ligated templates and unligated promoter strands. The polymerase is directed past the ligation site by adding ATP, GTP, and CTP. After washing away the NTPs, RNA transcripts are radiolabeled by adding α-^{32}P-GTP, then transcription is completed by addition of all four nucleotide triphosphates. RNA transcripts (dashed line) are analyzed by denaturing PAGE.

by washing the beads three times with TE300, and three times with transcription buffer (40 mM Tris-HCl [pH 7.9], 6 mM $MgCl_2$, 2 mM spermidine, 10 mM NaCl, and 10 mM DTT, in nuclease-free water). For transcription experiments, the beads were resuspended in 200 μl of transcription buffer for future use. For analysis of the ligation products, samples were incubated in 20 μl of 95% formamide, 25 mM EDTA at 90°C for 5 min to remove biotinylated DNA from the streptavidin constructs, and loaded directly onto a 6% urea-polyacrylamide gel for analysis (Figure S10).

Restriction Enzyme Mapping of Nucleosome Position

Details of restriction enzyme digestions of ligated templates are provided in Supplemental Experimental Procedures.

Single-Round In Vitro Transcription Assays with T7 RNA Polymerase

Single-round promoter-dependent transcription by T7 RNA polymerase was performed on the basis of two previously reported procedures, as shown in Figure 6 (Jung and Lippard, 2003; Walter and Studitsky, 2004). Immobilized DNA or NCP templates were pre-equilibrated with transcription buffer after ligation, as described in the previous section. Initial transcription walking past the promoter ligation site was performed in 20 μl of transcription buffer containing 25 nM DNA or NCP, 10 U T7 RNA polymerase, 1.0 U/μL RNasin (RNase inhibitor), 25 μM ATP, 25 μM GTP, and 25 μM CTP at room temperature for 5 min. Transcription stalls at the first dA in the template after synthesis of a 37 nt RNA transcript, because of the lack of UTP in solution. The supernatant was removed, and the immobilized transcription elongation complexes were washed five times each with 100 μl of reaction buffer. Radiolabeling of the RNA transcript was achieved by incubating the washed elongation complexes in 20 μl transcription buffer containing 1.0 U/μL RNasin, 1.0 μM UTP, and 0.6 μM α-^{32}P-GTP at room temperature for 5 min. This step allows the polymerase to incorporate the next 5 nt, including three ^{32}P-labeled GMP units, and stalls after synthesis of a 42-nt transcript. Finally, transcription was completed by addition of 0.5 mM NTPs to the solution and incubation for 15 min at room temperature, allowing the polymerase to transcribe off the template or release at any point along the DNA. Unlabeled GTP was present in 1000-fold excess in the final reaction solution, so subsequent rounds of transcription incorporate nonradiolabeled nucleotides and only the first round of RNA synthesis is visualized on a gel. The reaction was quenched by addition of an equal volume of 20 mM EDTA, and the supernatant was ethanol precipitated, dissolved in formamide, and analyzed by 6% urea-PAGE. For kinetic analysis, transcription was performed at 0°C, and aliquots of the final transcription solution were taken at 0, 15, 45, and 90 s for DNA templates, and at 0, 15, 30, 60, and 90 s for nucleosome templates.

ACCESSION NUMBERS

Structural coordinates have been deposited into the Protein Data Bank with accession code 3O62.

SUPPLEMENTAL INFORMATION

Supplemental Information includes ten figures, two tables, and Supplemental Experimental Procedures and can be found with this article online at doi:10.1016/j.chembiol.2010.10.018.

ACKNOWLEDGMENTS

This work was supported by the National Cancer Institute (grant CA034992 to S.J.L.). R.C.T. is grateful for fellowship support from the Koch Fund via the Koch Institute for Integrative Cancer Research. Portions of this research were conducted at the Advanced Photon Source on the Northeastern Collaborative Access Team beamlines, which are supported by award RR-15301 from the National Center for Research Resources at the National Institutes of Health. Use of the Advanced Photon Source is supported by the U.S. Department of Energy, Office of Basic Energy Sciences, under contract DE-AC02-06CH11357.

Received: July 29, 2010
Revised: October 6, 2010
Accepted: October 18, 2010
Published: December 21, 2010

REFERENCES

Bancroft, D.P., Lepre, C.A., and Lippard, S.J. (1990). ^{195}Pt NMR kinetic and mechanistic studies of *cis*- and *trans*-diamminedichloroplatinum(II) binding to DNA. J. Am. Chem. Soc. *112*, 6860–6871.

Bao, Y., White, C.L., and Luger, K. (2006). Nucleosome core particles containing a poly(dA·dT) sequence element exhibit a locally distorted DNA structure. J. Mol. Biol. *361*, 617–624.

Blommaert, F.A., van Dijk-Knijnenburg, H.C.M., Dijt, F.J., den Engelse, L., Baan, R.A., Berends, F., and Fichtinger-Schepman, A.M.J. (1995). Formation of DNA adducts by the anticancer drug carboplatin: different nucleotide sequence preferences in vitro and in cells. Biochemistry *34*, 8474–8480.

Bosl, G.J., and Motzer, R.J. (1997). Testicular germ-cell cancer. N. Engl. J. Med. *337*, 242–253.

Cohen, G.L., Ledner, J.A., Bauer, W.R., Ushay, H.M., Caravana, C., and Lippard, S.J. (1980). Sequence dependent binding of *cis*-dichlorodiammine-platinum(II) to DNA. J. Am. Chem. Soc. *102*, 2487–2488.

Danford, A.J., Wang, D., Wang, Q., Tullius, T.D., and Lippard, S.J. (2005). Platinum anticancer drug damage enforces a particular rotational setting of DNA in nucleosomes. Proc. Natl. Acad. Sci. USA *102*, 12311–12316.

Davey, C.A., Sargent, D.F., Luger, K., Maeder, A.W., and Richmond, T.J. (2002). Solvent mediated interactions in the structure of the nucleosome core particle at 1.9 Å resolution. J. Mol. Biol. *319*, 1097–1113.

Dhara, S.C. (1970). A rapid method for the synthesis of *cis*-$[Pt(NH_3)_2Cl_2]$. Indian J. Chem. *8*, 193–194.

Dyer, P.N., Edayathumangalam, R.S., White, C.L., Bao, Y., Chakravarthy, S., Muthurajan, U.M., and Luger, K. (2004). Reconstitution of nucleosome core particles from recombinant histones and DNA. Methods Enzymol. *375*, 23–44.

Flaus, A., and Owen-Hughes, T. (2001). Mechanisms for ATP-dependent chromatin remodelling. Curr. Opin. Genet. Dev. *11*, 148–154.

Galea, A.M., and Murray, V. (2002). The interaction of cisplatin and analogues with DNA in reconstituted chromatin. Biochim. Biophys. Acta *1579*, 142–152.

Galea, A.M., and Murray, V. (2010). The influence of chromatin structure on DNA damage induced by nitrogen mustard and cisplatin analogues. Chem. Biol. Drug Des. *75*, 578–589.

Gelasco, A., and Lippard, S.J. (1998). NMR solution structure of a DNA dodecamer duplex containing a *cis*-diammineplatinum(II) d(GpG) intrastrand cross-link, the major adduct of the anticancer drug cisplatin. Biochemistry *37*, 9230–9239.

Gottesfeld, J.M., Belitsky, J.M., Melander, C., Dervan, P.B., and Luger, K. (2002). Blocking transcription through a nucleosome with synthetic DNA ligands. J. Mol. Biol. *321*, 249–263.

Hayes, J.J., and Scovell, W.M. (1991). *cis*-Diamminedochloroplatinum(II) modified chromatin and nucleosome core particle probed with DNase I. Biochim. Biophys. Acta *1088*, 413–418.

He, B., Kukarin, A., Temiakov, D., Chin-Bow, S.T., Lyakhov, D.L., Rong, M., Durbin, R.K., and McAllister, W.T. (1998). Characterization of an unusual, sequence-specific termination signal for T7 RNA polymerase. J. Biol. Chem. *273*, 18802–18811.

Jamieson, E.R., and Lippard, S.J. (1999). Structure, recognition, and processing of cisplatin-DNA adducts. Chem. Rev. *99*, 2467–2498.

Jung, Y., and Lippard, S.J. (2003). Multiple states of stalled T7 RNA polymerase at DNA lesions generated by platinum anticancer agents. J. Biol. Chem. *278*, 52084–52092.

Jung, Y., and Lippard, S.J. (2007). Direct cellular responses to platinum-induced DNA damage. Chem. Rev. *107*, 1387–1407.

Kartalou, M., and Essigmann, J.M. (2001). Mechanisms of resistance to cisplatin. Mutat. Res. *478*, 23–43.

Keys, H.M., Bundy, B.N., Stehman, F.B., Muderspach, L.I., Chafe, W.E., Suggs, C.L., III, Walker, J.L., and Gersell, D. (1999). Cisplatin, radiation, and adjuvant hysterectomy compared with radiation and adjuvant hysterectomy for bulky stage IB cervical carcinoma. N. Engl. J. Med. *340*, 1154–1161.

Kireeva, M.L., Walter, W., Tschernajenko, V., Bondarenko, V.A., Kashlev, M., and Studitsky, V.M. (2002). Nucleosome remodeling induced by RNA polymerase II: loss of the H2A/H2B dimer during transcription. Mol. Cell *9*, 541–552.

Kirov, N., Tsaneva, I., Einbinder, E., and Tsanev, R. (1992). In vitro transcription through nucleosomes by T7 RNA polymerase. EMBO J. *11*, 1941–1947.

Kornberg, R.D., and Lorch, Y. (1999). Twenty-five years of the nucleosome, fundamental particle of the eukaryote chromosome. Cell *98*, 285–294.

Lavery, R., Moakher, M., Maddocks, J.H., Petkeviciute, D., and Zakrzewska, K. (2009). Conformational analysis of nucleic acids revisited: Curves+. Nucleic Acids Res. *37*, 5917–5929.

Lippard, S.J., and Hoeschele, J.D. (1979). Binding of *cis*- and *trans*-dichlorodiammineplatinum(II) to the nucleosome core. Proc. Natl. Acad. Sci. USA *76*, 6091–6095.

Loehrer, P.J., and Einhorn, L.H. (1984). Drugs five years later: cisplatin. Ann. Intern. Med. *100*, 704–713.

Luger, K., Mäder, A.W., Richmond, R.K., Sargent, D.F., and Richmond, T.J. (1997). Crystal structure of the nucleosome core particle at 2.8 Å resolution. Nature *389*, 251–260.

Luger, K. (2006). Dynamic nucleosomes. Chromosome Res. *14*, 5–16.

Macdonald, L.E., Zhou, Y., and McAllister, W.T. (1993). Termination and slippage by bacteriophage T7 RNA polymerase. J. Mol. Biol. *232*, 1030–1047.

Mohammad-Rafiee, F., Kulić, I.M., and Schiessel, H. (2004). Theory of nucleosome corkscrew sliding in the presence of synthetic DNA ligands. J. Mol. Biol. *344*, 47–58.

Morris, M., Eifel, P.J., Lu, J., Grigsby, P.W., Levenback, C., Stevens, R.E., Rotman, M., Gershenson, D.M., and Mutch, D.G. (1999). Pelvic radiation and concurrent chemotherapy compared with pelvic and para-aortic radiation for high-risk cervical cancer. N. Engl. J. Med. *340*, 1137–1143.

Mymryk, J.S., Zaniewski, E., and Archer, T.K. (1995). Cisplatin inhibits chromatin remodeling, transcription factor binding, and transcription from the mouse mammary tumor virus promoter in vivo. Proc. Natl. Acad. Sci. USA *92*, 2076–2080.

Nacheva, G.A., and Berzal-Herranz, A. (2003). Preventing nondesired RNA-primed RNA extension catalyzed by T7 RNA polymerase. Eur. J. Biochem. *270*, 1458–1465.

Ober, M., and Lippard, S.J. (2007). Cisplatin damage overrides the predefined rotational setting of positioned nucleosomes. J. Am. Chem. Soc. *129*, 6278–6286.

Ober, M., and Lippard, S.J. (2008). A 1,2-d(GpG) cisplatin intrastrand cross-link influences the rotational and translational setting of DNA in nucleosomes. J. Am. Chem. Soc. *130*, 2851–2861.

Park, Y.-J., Chodaparambil, J.V., Bao, Y., McBryant, S.J., and Luger, K. (2005). Nucleosome assembly protein 1 exchanges histone H2A-H2B dimers and assists nucleosome sliding. J. Biol. Chem. *280*, 1817–1825.

Pennings, S., Meersseman, G., and Bradbury, E.M. (1991). Mobility of positioned nucleosomes on 5 S rDNA. J. Mol. Biol. *220*, 101–110.

Reinberg, D., and Sims, R.J., III. (2006). deFACTo nucleosome dynamics. J. Biol. Chem. *281*, 23297–23301.

Rong, M., Durbin, R.K., and McAllister, W.T. (1998). Template strand switching by T7 RNA polymerase. J. Biol. Chem. *273*, 10253–10260.

Rosenberg, B., Van Camp, L., and Krigas, T. (1965). Inhibition of cell division in *Escherichia coli* by electrolysis products from a platinum electrode. Nature *205*, 698–699.

Rosenberg, B., Van Camp, L., Trosko, J.E., and Mansour, V.H. (1969). Platinum compounds: a new class of potent antitumour agents. Nature *222*, 385–386.

Schenborn, E.T., and Mierendorf, R.C., Jr. (1985). A novel transcription property of SP6 and T7 RNA polymerases: dependence on template structure. Nucleic Acids Res. *13*, 6223–6236.

Segal, E., Fondufe-Mittendorf, Y., Chen, L., Thåström, A., Field, Y., Moore, I.K., Wang, J.-P.Z., and Widom, J. (2006). A genomic code for nucleosome positioning. Nature *442*, 772–778.

Studitsky, V.M., Clark, D.J., and Felsenfeld, G. (1994). A histone octamer can step around a transcribing polymerase without leaving the template. Cell *76*, 371–382.

Studitsky, V.M., Clark, D.J., and Felsenfeld, G. (1995). Overcoming a nucleosomal barrier to transcription. Cell *83*, 19–27.

Studitsky, V.M., Kassavetis, G.A., Geiduschek, E.P., and Felsenfeld, G. (1997). Mechanism of transcription through the nucleosome by eukaryotic RNA polymerase. Science *278*, 1960–1963.

Teuben, J.-M., Bauer, C., Wang, A.H.-J., and Reedijk, J. (1999). Solution structure of a DNA duplex containing a *cis*-diammineplatinum(II) 1,3-d(GTG) intrastrand cross-link, a major adduct in cells treated with the anticancer drug carboplatin. Biochemistry *38*, 12305–12312.

Thåström, A., Lowary, P.T., and Widom, J. (2004). Measurement of histone-DNA interaction free energy in nucleosomes. Methods *33*, 33–44.

Todd, R.C., and Lippard, S.J. (2009). Inhibition of transcription by platinum antitumor compounds. Metallomics *1*, 280–291.

Walter, W., and Studitsky, V.M. (2004). Construction, analysis, and transcription of model nucleosomal templates. Methods *33*, 18–24.

Wang, D., Hara, R., Singh, G., Sancar, A., and Lippard, S.J. (2003). Nucleotide excision repair from site-specifically platinum-modified nucleosomes. Biochemistry *42*, 6747–6753.

Wang, D., and Lippard, S.J. (2005). Cellular processing of platinum anticancer drugs. Nat. Rev. Drug Discov. *4*, 307–320.

Workman, J.L. (2006). Nucleosome displacement in transcription. Genes Dev. *20*, 2009–2017.

Wu, B., and Davey, C.A. (2008). Platinum drug adduct formation in the nucleosome core alters nucleosome mobility but not positioning. Chem. Biol. *15*, 1023–1028.

Wu, B., Dröge, P., and Davey, C.A. (2008). Site selectivity of platinum anticancer therapeutics. Nat. Chem. Biol. *4*, 110–112.